

Investigation of Two Plane Parallel Jets

H. Elbanna* and S. Gahin†

King Abdulaziz University, Jeddah, Saudi Arabia

and

M. I. I. Rashed‡

Cairo University, Cairo, Egypt

Results of an experimental study on the interaction of two two-dimensional turbulent parallel jets are reported. The investigation includes measurements of mean velocity, turbulence intensities, and Reynolds shear stress. The structure of the combined flow is compared with that of a single jet. The results show that the velocity profiles of the combined flow are similar and agree well with that of the single jet. Up to 120 slot widths downstream from the nozzles, true similarity is not found. For a spacing of 12.5 slot widths between the axes of the two nozzles, the half-width of the combined flow grows linearly with downstream distance, but its spread angle is slightly lower than that of a single jet. The centerline velocity decays with the same rate as the single jet, but with a higher value of U_M/U_0 .

Nomenclature

S	= spacing between the two nozzles
t_p	= jet nozzle width
\bar{U}	= mean velocity in the x direction
u, v, w	= fluctuating velocity components along x , y , and z , respectively
u', v', w'	= rms of fluctuating velocity components along x , y , and z , respectively
uv	= Reynolds shear stress
x	= streamwise coordinate along centerline
y	= coordinate normal to the centerline
$y_{0.5}$	= half-width of the mean velocity profile along the y axis
z	= coordinate normal to floor and ceiling planes
η	= dimensionless distance y/x

Subscripts

M	= centerline conditions
max	= maximum value
0	= nozzle exit plane conditions

Introduction

THE turbulent mixing of jets can be applied in a wide variety of fields. It is used, for example, in burners and in thrust-augmenting ejectors for VTOL and STOL aircraft. The flow configuration of interest here is that shown in Fig. 1. Two identical two-dimensional jets of air issue from parallel free-standing nozzles. Mutual entrainment of the surrounding fluid creates a subatmospheric region between the two jets. For this reason, the two jets attract each other and finally merge together to form a single jet. The flowfield generated by two plane parallel jets issuing from parallel slot nozzles in a common wall has been examined experimentally.^{1,4} The work of Marsters⁵ is perhaps the only case reported in the literature for jets issuing from free-standing (ventilated) nozzles. In this case, interjet air entrainment is allowed and the formation of vortices upstream of the merging region is not observed. Marsters' work⁵ included measurements of static pressure and mean velocities and was not concerned with turbulence intensities.

The characteristics of the flowfield are influenced by the spacing between the two nozzles S , see Fig. 1. In the present investigation, S has the value of 12.5 slot widths t_p . Measurements were made up to 120 times t_p downstream from the nozzles. They included mean velocities, turbulent intensities for the rms of the three fluctuating velocity components u' , v' , and w' and Reynolds shear stress.

Experimental Apparatus

The apparatus used is shown schematically in Fig. 2. Two variable-speed centrifugal fans were used to provide the airflow to two identical separate nozzle blocks. The width of the nozzle slot t_p is 1.2 cm and its height is 49 cm. Before reaching the slot, the air passes through a settling chamber which contains three screens to produce a uniform velocity along the length of the slot. The nozzle blocks are held between two horizontal walls extending 200 cm downstream of the slots and 100 cm on each side of the midline between the two nozzles. The facility is designed such that each of the two nozzle blocks can be rotated around the vertical axis of the slot for further experiments on the intercepting jets. The design allows the jet to span all of the distance between the floor and ceiling confining walls. Several measurements were carried out to assure two-dimensionality. Over the central 38 cm of the distance between the floor and ceiling walls, the velocity at nozzle exit was highly uniform and even at a downstream distance, $x=120t_p$, the variation in total head did not exceed 2.4%. The exit Reynolds number was 2×10^4 and the turbulence level was 1%. The traversing mechanism enabled the measuring instrument to be traversed longitudinally in the downstream direction and laterally across the jet. The apparatus is placed in nearly symmetric position of a large air-conditioned room. The distance from the apparatus boundary to the nearest wall was greater than 5 m.

Instrumentation and Procedure

Measurements were made with DISA 55M-01 constant temperature anemometers in conjunction with DISA 55-M25 linearizers. The linearizers were calibrated with the aid of DISA 55-D90 calibration equipment. An automatic X-Y recorder was used for plotting calibration curves. Most of the measurements were made using either symmetric X-wire or a single inclined wire. The probes were manufactured by DISA and constructed from 5 μ m platinum-coated tungsten wire with an active length of 1.25 mm. The distance between the two wires of the X-wire probe is of the order of one wire length. Jerome et al.⁶ had shown that for such a distance, the thermal wake effects on X-wire measurements are avoided

Received April 30, 1982; revision received Nov. 1, 1982. Copyright © American Institute of Aeronautics and Astronautics, Inc., 1982. All rights reserved.

*Lecturer, Department of Mechanical Engineering.

†Professor, Department of Mechanical Engineering.

‡Professor, Department of Aeronautical Engineering.

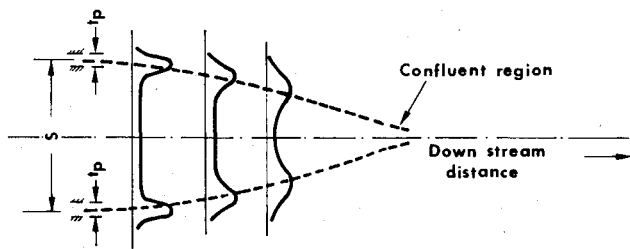


Fig. 1 Flow configuration of two turbulent parallel jets.

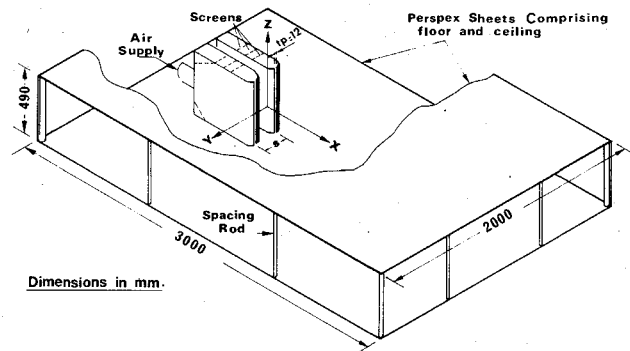


Fig. 2 Schematic diagram of experimental apparatus.

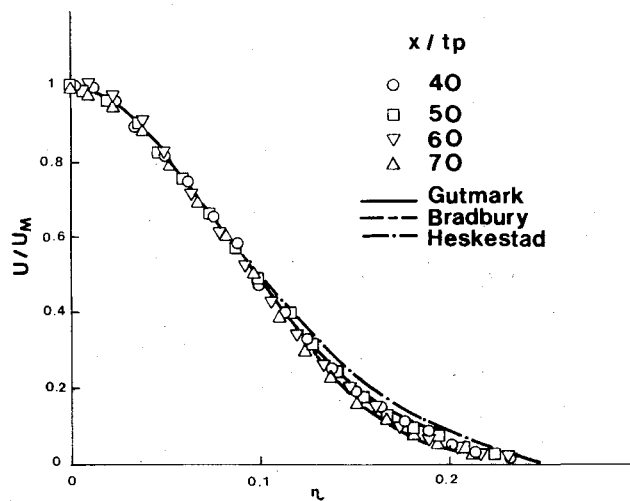


Fig. 3 Velocity profile for the single jet.

and the wire can be considered to have no pitch sensitivity. The X-wire probe can be used in oblique operation for measuring mean velocities and the three component turbulent intensities with adequate accuracy⁷⁻⁹ up to an angle of 25 deg. For the Reynolds shear stress higher errors are obtained with oblique operation.⁷

The calibration equipment together with the X-Y recorder has enabled calibration to be conducted easily before each run and to be checked and readjusted at the beginning of each lateral traverse. Measurements of correlations were made using DISA 52-B25 turbulence processor. Mean values and rms values were obtained using DISA 55-D31 digital voltmeters and DISA 55-D35 rms units, respectively. Most of these instruments have integration times of 0.1-100 s. In the present investigation, averaging times of 30 s were used in the outer portions of the jet and 10 s in the rest of the flowfield.

Summary of Single-Jet Measurements

Mean Velocity

For convenience in comparison of results, the single jet was investigated and compared with the results of previous in-

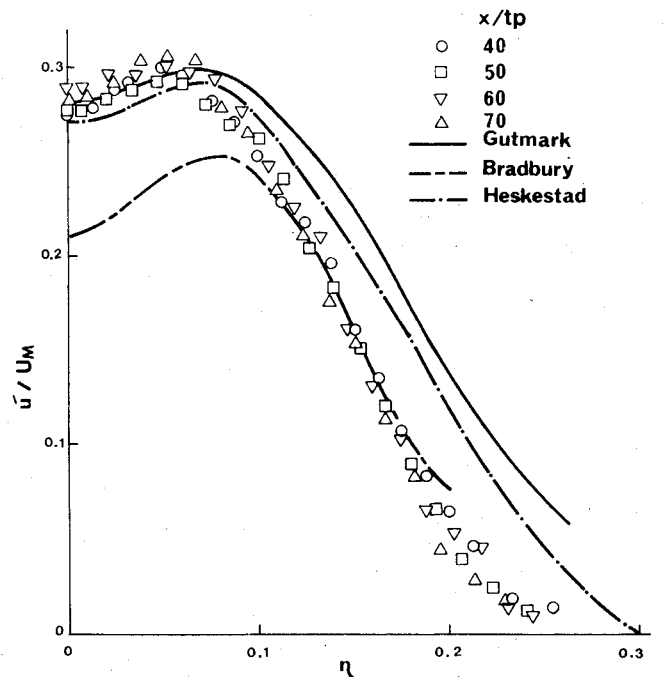


Fig. 4 Distribution of the axial velocity fluctuations for the single jet.

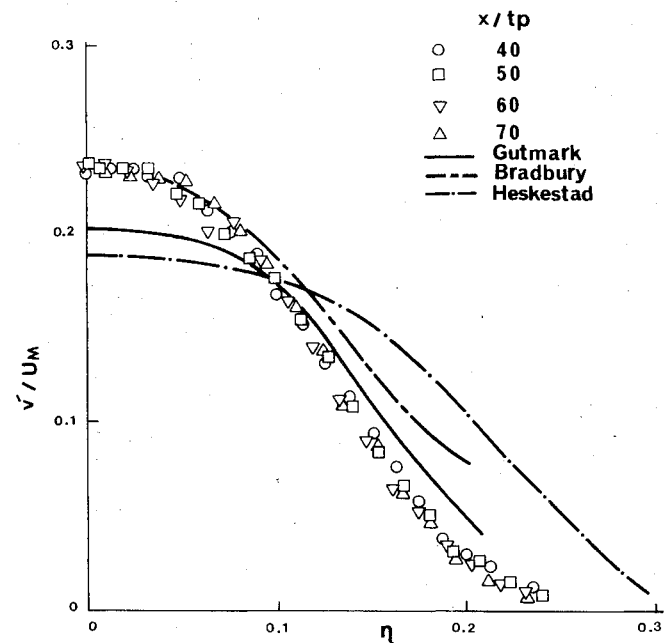


Fig. 5 Distribution of the lateral velocity fluctuations for the single jet.

vestigators.¹⁰⁻¹² Mean velocity profiles normalized by the maximum velocity at a given value of x/t_p are shown in Fig. 3. The profiles exhibit good similarity and have the usual bell shape. The agreement between the present results and that of Gutmark,¹⁰ Bradbury,¹¹ and Heskestad¹² is very good for $\eta < 0.1$. Near the edge, the four sets of data appear to be somewhat different, probably due to the measuring accuracy in this low-velocity region.

Turbulence Quantities

The rms fluctuating velocity components u' , v' , and w' are shown in Figs. 4-6, along with the results of Refs. 10-12. The distribution of Reynolds shear stress \overline{uv} is shown in Fig. 7. Agreement between the four sets of results is poor. One may attribute this difference to the influence of the apparatus design and initial conditions at the nozzle exit.¹³

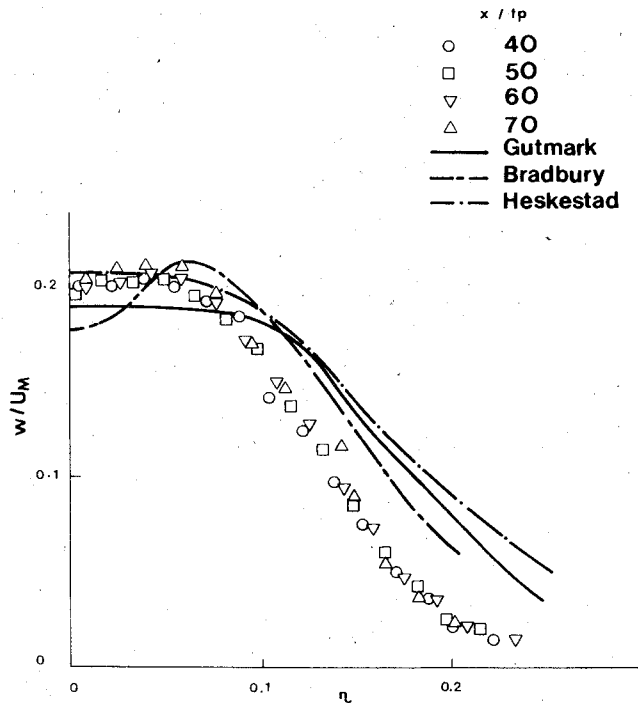


Fig. 6 Distribution of the transverse velocity fluctuations for the single jet.

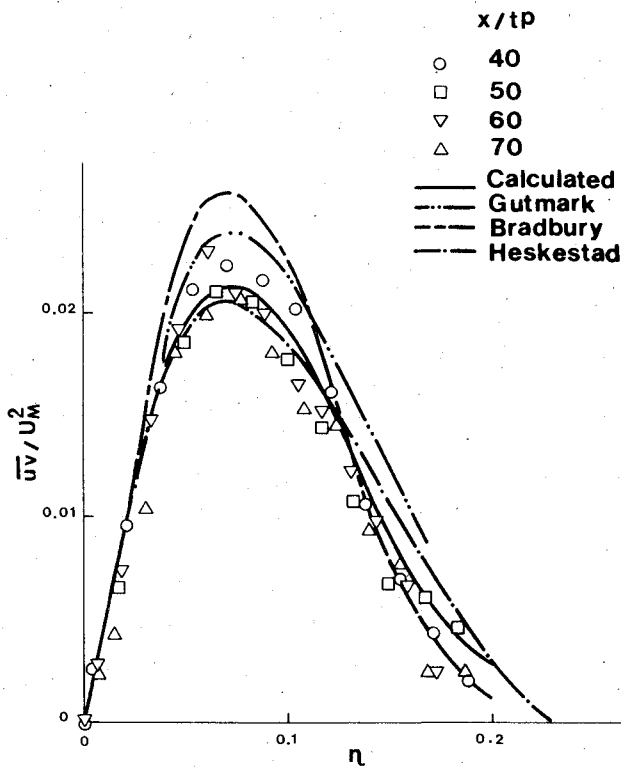


Fig. 7 Distribution of the turbulent shear stress for the single jet.

The distribution of the axial velocity fluctuations u'/U_M compares favorably with that of Gutmark¹⁰ and Heskestad¹² for $\eta < 0.1$. But for $\eta > 0.1$, the present results are in good agreement with those of Bradbury¹¹ but substantially lower than those of Gutmark and Heskestad. In the present experiment as in Bradbury's experiment, the apparatus design allows the entrained streamlines to be approximately parallel to the axis of the jet. This has the advantage of decreasing the turbulent intensities at the edge of the jet and leads to more accurate measurements.

The distribution of the lateral velocity fluctuations v'/U_M is shown in Fig. 5. In the central part of the jet the v' profile agrees well with that observed by Bradbury. But in the outer region of the jet, the present results are nearer to those of Gutmark.

In Fig. 6, the distribution of the transverse velocity fluctuations w'/U_M is shown. In the central part of the jet, the present results are closer to those of Heskestad except that the present distribution shows a slight "saddle-back" shape which was observed only in Bradbury's results. However, the ratio w'_{max}/w'_M takes the value of 1.05 and 1.2 for the present and Bradbury's results, respectively. In the outer part of the jet, the transverse velocity fluctuations are lower than those measured by Gutmark, Bradbury, and Heskestad.

The measured distribution of the turbulent shear stress $\bar{u}v$ is shown in Fig. 7. Good agreement is obtained between the measured values and the distribution calculated from the mean velocity profile by neglecting the normal stresses. The maximum value of the shear stress occurs at around $\eta = 0.07$.

Characteristics of the Flowfield of the Two Jets

Mean Velocity

Figure 8 shows the distribution of velocity along the y axis at $x/t_p = 1, 4, 7, \text{ and } 15$. The velocity is normalized with respect to the velocity at nozzle exit, while the y coordinate is normalized with respect to the spacing S between the two nozzles. As seen, the maximum velocity of the jet and its location from the x axis decrease with the distance from the nozzle. The two jets finally approach the x axis and join to form a single jet. The entrained secondary flow between the two jets is clearly noticeable. The distribution of velocity along the x axis is shown in Fig. 9. At the centerline, the ratio of the secondary flow velocity to the exit velocity U/U_0 has the value 0.15 at $x/t_p = 1$ and decreases with x/t_p up to a value of about 0.04 at $x/t_p = 12$. For $x/t_p > 12$, the centerline velocity begins to rise with x/t_p up to a maximum value in the region where the two jets join together at x/t_p around 30. The ratio U_M/U_0 for the combined jet is higher than that for the single jet and decays at nearly the same rate as the single jet.

Figure 10 shows the velocity profiles in the combined jet. In this case the y coordinate is normalized with respect to $y_{0.5}$. The profiles are similar and have the shape of those of the single jet. Figure 11 shows the growth of the half-width of the combined jet. As shown in the figure, the half-width $y_{0.5}$ grows linearly with x/t_p . However, its spread angle is slightly lower than that of the single jet. The lower spread rate may be

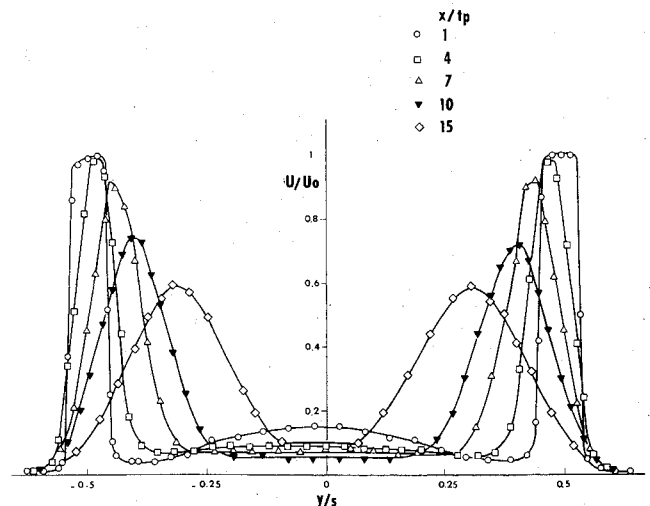


Fig. 8 Mean velocity distribution upstream of the merging region of the two parallel jets.

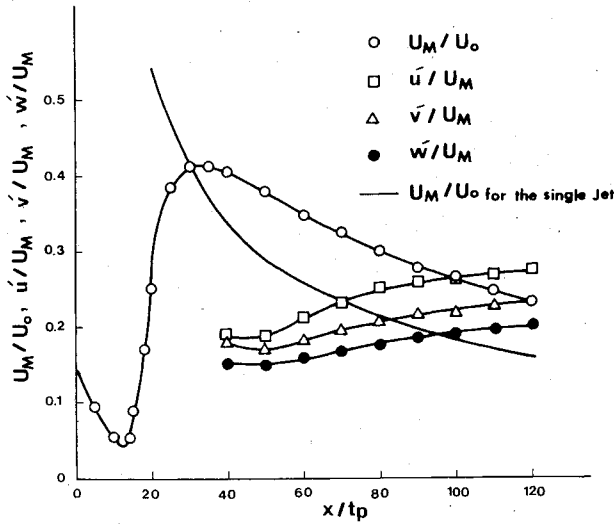


Fig. 9 Variation of mean velocity and turbulent intensities along the centerline of the parallel jets.

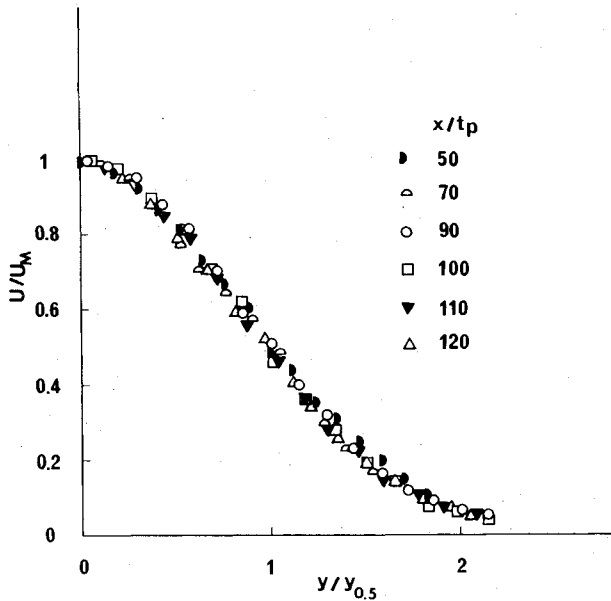


Fig. 10 Velocity profile for the combined parallel jets.

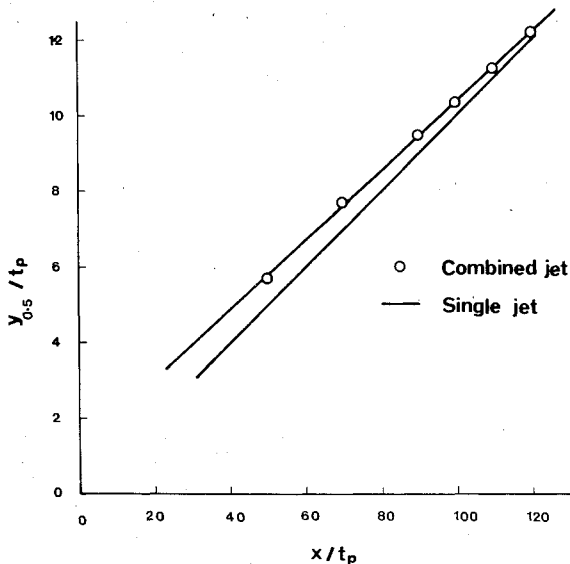


Fig. 11 Growth of the combined jet with downstream distance.

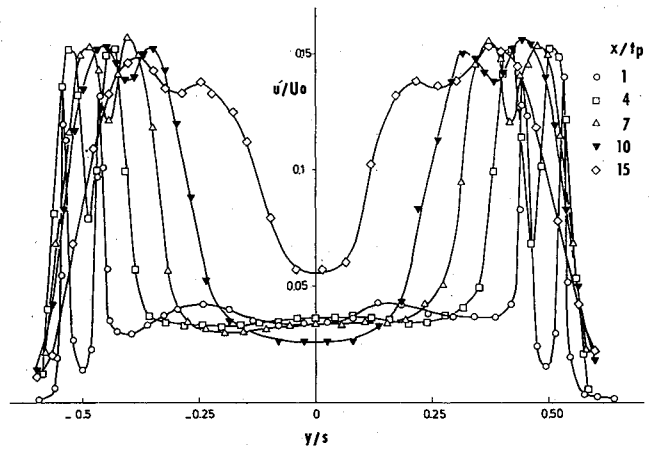


Fig. 12 Distribution of the axial velocity fluctuations upstream of the merging region of the two parallel jets.

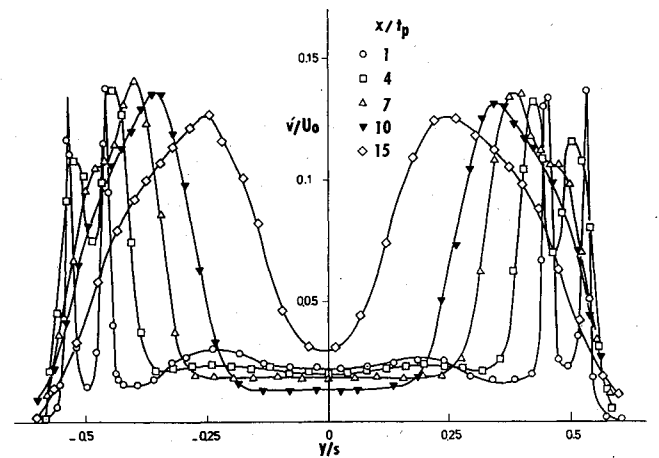


Fig. 13 Distribution of the lateral velocity fluctuations upstream of the merging region of the two parallel jets.

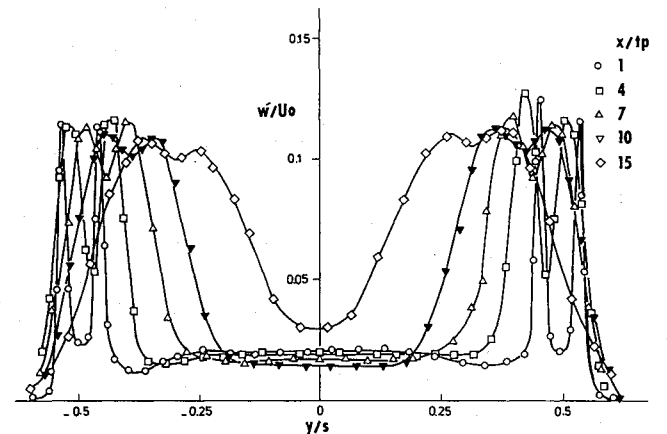


Fig. 14 Distribution of the transverse velocity fluctuations upstream of the merging region of the two parallel jets.

attributed to the streaming effect of the entrainment fluid. This effect should depend upon the geometrical parameters of the flowfield, in particular, the spacing S and the dimensions of the bounding plates.

Turbulence Quantities

The distribution of the turbulent intensities along the centerline is shown in Fig. 9. The figure shows that in this investigation, the three components of the turbulent intensities still rise with the axial distance up to $x/t_p = 120$. The

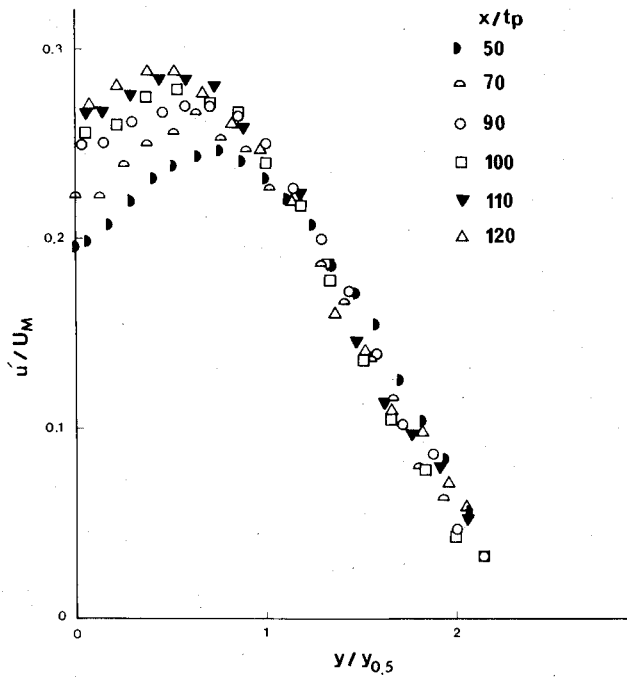


Fig. 15 Distribution of the axial velocity fluctuations for the combined jet.

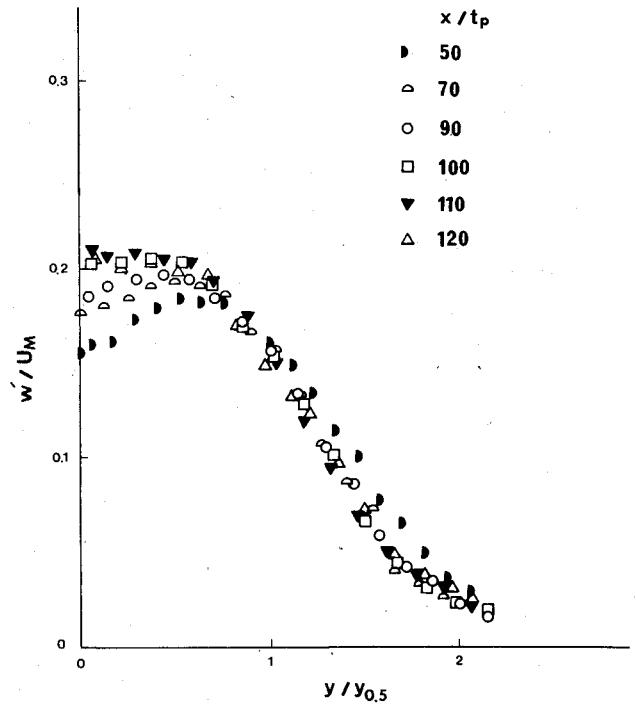


Fig. 17 Distribution of the transverse velocity fluctuations for the combined jet.

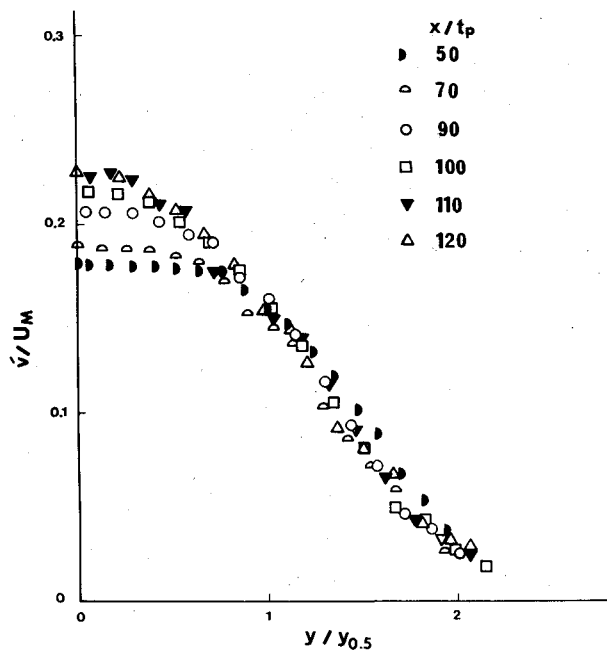


Fig. 16 Distribution of the lateral velocity fluctuations for the combined jet.

distribution of the u' , v' , and w' components upstream of the merging region are shown in Figs. 12-14. From these figures, it is seen that near the nozzle exit, the maximum values of the velocity fluctuations u'/U_0 , v'/U_0 , and w'/U_0 exist in positions corresponding to the nozzle edges, while the minimum values correspond to the axis of each jet and the secondary flow.

The distribution of the turbulent velocity fluctuations downstream of the merging region u'/U_M , v'/U_M , and w'/U_M are presented in Figs. 15-17. Figure 15 shows that the profiles of the axial velocity fluctuations u'/U_M are not similar and have the "saddle-back" shape. At $x/t_p = 50$, the maximum value of u' occurs at $y/y_{0.5} = 0.76$. As x/t_p increases, the magnitude of this maximum increases and its

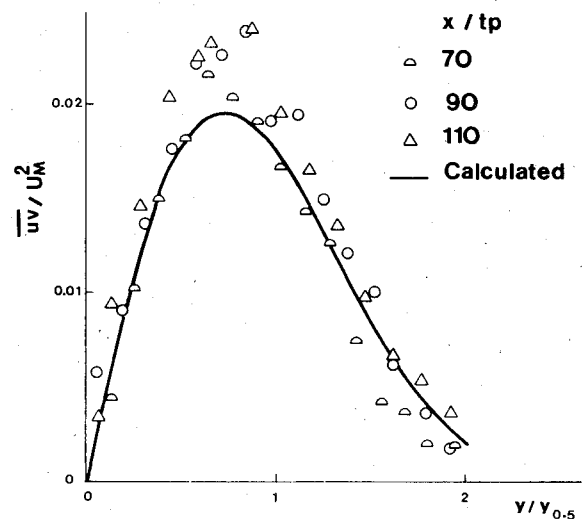


Fig. 18 Distribution of the turbulent shear stress for the combined jet.

location moves toward the centerline. Also, the value of the ratio u'_{max}/u'_M is quite large near the confluent region, indicating the effects of the merging of the two shear layers at the outside of the combined jet.

As shown in Fig. 16, the maximum value of the lateral velocity fluctuations v'/U_M occurs at the centerline and its magnitude increases with x/t_p . Figure 17 shows that the distribution of the transverse velocity fluctuations w'/U_M exhibits the "saddle-back" shape at lower values of x/t_p , but as x/t_p increases, this shape gradually disappears. For $x/t_p = 50$, the location of w'_{max} occurs at $y/y_{0.5} = 0.58$ and moves toward the centerline as x/t_p increases.

The variation of the turbulent shear stress uv is shown in Fig. 18 together with the distribution calculated from the mean velocity profile. The maximum value of the shear stress is about the same as the single jet and occurs at around $y/y_{0.5} = 0.8$. However, the maximum measured value of uv is about 13% higher than the calculated one.

Conclusions

The following conclusions can be drawn from the experimental results presented in this paper of the mixing between two plane parallel ventilated jets:

- 1) The velocity profiles of the combined flow are similar and agree well with that of the single jet.
- 2) The centerline velocity decays with the same rate as for the single jet, but with higher value of U_M/U_0 .
- 3) The width of the combined jet spreads linearly downstream as a single jet, but its spread angle is slightly lower.
- 4) The distributions of the three components of turbulent velocity fluctuations show different behavior than that for the single jet and true similarity was not observed up to $x/l_p = 120$.
- 5) The maximum shear stress has nearly the same value as that in the single jet.

Acknowledgments

This paper presents part of the experimental results obtained in a research project on Oil Well Fire Fighting (OWFF) sponsored by the Ministry of Petroleum and Minerals of Saudi Arabia. The authors are very grateful to Prof. G. Elsabbagh and Dr. A.M.A. Khalifa of the Mechanical Engineering Department, King Abdulaziz University, for their fruitful discussions throughout the course of this investigation.

References

¹Tanaka, E., "The Interference of Two-Dimensional Parallel Jets (1st Rept.)," *Bulletin of the JSME*, Vol. 13, No. 56, 1970, pp. 272-280.

²Tanaka, E., "The Interference of Two-Dimensional Parallel Jets (2nd Rept.)," *Bulletin of the JSME*, Vol. 17, No. 109, 1974, pp. 920-927.

³Miller, D. R. and Comings, E. W., "Force-Momentum Fields in a Dual-Jet Flow," *Journal of Fluid Mechanics*, Vol. 7, Feb. 1960, pp. 237-256.

⁴Murai, K., Taga, M., and Akagaw, K., "An Experimental Study on Confluence of Two Two-Dimensional Jets," *Bulletin of the JSME*, Vol. 19, No. 134, 1976, pp. 958-964.

⁵Marsters, G. F., "Interaction of Two Plane, Parallel Jets," *AIAA Journal*, Vol. 15, Dec. 1977, pp. 1756-1762.

⁶Jerome, F. E., Guitton, D. E., and Patel, R. P., "Experimental Study of the Thermal Wake Interference Between Closely Spaced Wires of a X-Type Hot-Wire Probe," *Aeronautical Quarterly*, Vol. 23, May 1971, pp. 119-126.

⁷Klatt, F., "The X Hot-Wire Probe in a Plane Flow Field," *DISA Information*, No. 8, July 1969, pp. 3-11.

⁸Bruun, H. H., "Interpretation of X-Hot-Wire Signals," *DISA Information*, No. 18, Sept. 1975, pp. 5-10.

⁹Korthapalli, A., Baganoff, D., and Karamcheti, K., "Development and Structure of a Rectangular Jet in a Multiple Jet Configuration," *AIAA Journal*, Vol. 15, Aug. 1980, pp. 945-950.

¹⁰Gutmark, E. and Wagnaski, I., "The Planar Turbulent Jet," *Journal of Fluid Mechanics*, Vol. 73, Pt. 3, 1976, pp. 465-495.

¹¹Bradbury, L. J. S., "The Structure of a Self Preserving Turbulent Plane Jet," *Journal of Fluid Mechanics*, Vol. 23, Pt. 1, 1965, pp. 31-64.

¹²Heskestad, G., "Hot Wire Measurements in a Plane Turbulent Jet," *Transactions of ASME, Journal of Applied Mechanics*, Vol. 32, Dec. 1965, pp. 721-734.

¹³Rodi, W., "A Review of Experimental Data of Uniform Density Free Turbulent Boundary Layers," *Studies in Convection, Theory, Measurements and Applications*, edited by B. E. Launder, Academic Press, New York, 1975, pp.79-165.

From the AIAA Progress in Astronautics and Aeronautics Series..

RAREFIED GAS DYNAMICS: PART I AND PART II—v. 51

Edited by J. Leith Potter

Research on phenomena in rarefied gases supports many diverse fields of science and technology, with new applications continually emerging in hitherto unexpected areas. Classically, theories of rarefied gas behavior were an outgrowth of research on the physics of gases and gas kinetic theory and found their earliest applications in such fields as high vacuum technology, chemical kinetics of gases, and the astrophysics of interstellar media.

More recently, aerodynamicists concerned with forces on high-altitude aircraft, and on spacecraft flying in the fringes of the atmosphere, became deeply involved in the application of fundamental kinetic theory to aerodynamics as an engineering discipline. Then, as this particular branch of rarefied gas dynamics reached its maturity, new fields again opened up. Gaseous lasers, involving the dynamic interaction of gases and intense beams of radiation, can be treated with great advantage by the methods developed in rarefied gas dynamics. Isotope separation may be carried out economically in the future with high yields by the methods employed experimentally in the study of molecular beams.

These books offer important papers in a wide variety of fields of rarefied gas dynamics, each providing insight into a significant phase of research.

Volume 51 sold only as a two-volume set
Part I, 658 pp., 6x9, illus.
Part II, 679 pp., 6x9, illus.
\$37.50 Member, \$70.00 List

TO ORDER WRITE: Publications Dept., AIAA, 1290 Avenue of the Americas, New York, N.Y. 10019